

Peptide hydrolysis and uptake of peptide hydrolysis products in the James River estuary and lower Chesapeake Bay

Tiantian Tang^{a,b,*}, Katherine C. Filippino^c, Zhanfei Liu^{d,e}, Margaret R. Mulholland^c, Cindy Lee^a

^a School of Marine and Atmospheric Sciences, Stony Brook University, Stony Brook, NY 11794-5000, United States

^b State Key Laboratory of Marine Environmental Science, Xiamen University, Xiamen, 361005, China

^c Department of Ocean, Earth and Atmospheric Sciences, Old Dominion University, Norfolk, VA 23529-0126, United States

^d Department of Chemistry, Old Dominion University, Norfolk, VA 23529-0126, United States

^e Marine Science Institute, University of Texas at Austin, Port Aransas, TX 78373-5015, United States

ARTICLE INFO

Keywords:

Extracellular peptide hydrolysis
Dissolved combined amino acids
Dissolved free amino acids
Dissolved organic matter
Dissolved organic nitrogen
Nitrogen uptake
Chesapeake Bay
James River

ABSTRACT

The lability of small peptides was investigated along the salinity gradient of the James River estuary and lower Chesapeake Bay using two fluorescent analogs, Lucifer Yellow Anhydride-alanine-valine-phenylalanine-alanine (LYA-AVFA) and LYA-tetraalanine (LYA-ALA₄). Hydrolysis rates of these compounds were compared with each other, and with uptake rates of potential hydrolysis products and other smaller derivatives (e.g., glutamic acid and dialanine). Results suggest that rates of peptide hydrolysis and uptake of hydrolysis products were not always correlated with each other along the salinity gradient, or to other environmental parameters measured in the James River and lower Chesapeake Bay. This may be because diverse input and removal processes can influence both peptide hydrolysis and uptake, but not necessarily simultaneously. Rates of both peptide hydrolysis and free amino acid uptake were strongly associated with particles, particularly those freshly produced. This suggests more rapid turnover of enzymatically available organic nitrogen in regions with elevated phytoplankton biomass. Changes in the abundance and composition of dissolved amino acids in these waters were also examined. Dissolved amino acid compositions, but not concentrations, varied with salinity along a gradient from the tidal fresh James River to the mouth of Chesapeake Bay. These compositional variations demonstrate the mixing of terrestrial organic nitrogen and in-situ production along the salinity transect.

1. Introduction

Total hydrolyzable amino acids (THAA) are one of the most abundant classes of dissolved organic matter (DOM) produced by marine organisms, but due to their rapid degradation rates and bioavailability (Coffin, 1989; Kroer et al., 1994; Mulholland and Lomas, 2008), they represent only 0.4–4% of dissolved organic carbon (DOC) and 1.4–11% of dissolved organic nitrogen (DON) in the water column (Bronk, 2002; Repeta, 2014). Dissolved free amino acids (DFAA) account for only a small fraction of THAA (Keil and Kirchman, 1991); the rest are in the form of combined amino acids (DCAA). The abundances and molecular compositions of DCAA and DFAA vary greatly among marine environments due to their multiple production and decomposition pathways (Keil and Kirchman, 1991; Yamashita and Tanoue, 2003; Kuznetsova et al., 2004). A variety of biotic and abiotic processes contribute to the input, transport, and removal of DFAA and DCAA in coastal regions. These include river runoff, phytoplankton growth, respiration of

organic matter, sediment resuspension and photodegradation (Guldberg et al., 2002; Hoppe et al., 2002; Rosenstock et al., 2005; Grace and Bianchi, 2010; Arnosti, 2011). In particular, dissolved amino acids are sources of energy and nutrients for both heterotrophic and autotrophic microorganisms. Uptake of DFAA by heterotrophic bacteria (Williams et al., 1976; Billen and Fontigny, 1987; Fuhrman, 1987; Berman and Bronk, 2003) and phytoplankton (Mulholland et al., 2002; Mulholland and Lomas, 2008) is well documented in natural waters. However, DCAA, the largest pool of dissolved amino acids, are thought to be less available to most microorganisms because molecules larger than about 600 Da cannot pass through cell membranes (Payne, 1980; Weiss et al., 1991). Recent studies have shown that microbial communities can take up not only DFAA but also dipeptides (Kirchman and Hodson, 1984; Mulholland and Lee, 2009). However, extracellular hydrolysis of peptides into components small enough to be taken up appears to be the rate-limiting step in the use of DCAA by microbes (Chrost, 1991), and the extent to which enzymatic hydrolysis limits the

* Corresponding author.

E-mail address: tiantian.tang@xmu.edu.cn (T. Tang).

¹ Current address: State Key Laboratory of Marine Environmental Science, Xiamen University, Xiamen 361005, China.

use of DCAA is likely complex and varied in diverse aquatic environments (Arnosti, 2004).

Although it is known that peptide bonds are commonly produced during biologically mediated metabolism, our understanding of their biogeochemical importance in aquatic ecosystems is incomplete. Peptide hydrolysis has long been investigated using synthetic analogs of peptides, including fluorescently-labeled and isotopically-labeled amino acids and small peptides (e.g., Hollibaugh and Azam, 1983; Hoppe, 1983; Somville and Billen, 1983). The advantage of using fluorescent analogs instead of native compounds is that analytical detection limits of fluorescent analogs are much lower than those of the native compounds; additions as low as 5 nmol L^{-1} , which is close to amino acid concentrations in natural aquatic environments, can be used. Fluorescent analogs also tend to be much cheaper and safer to use than ^{14}C or ^3H -labeled compounds. Peptides labeled with the fluorochrome Lucifer Yellow Anhydride (LYA) allow measurement of hydrolysis rate constants of actual peptides as well as identification of hydrolysis products (Pantoja et al., 1997). Using this technique, peptide hydrolysis has been evaluated in estuaries (Mulholland et al., 2002, 2003; Mulholland and Lee, 2009), surface microlayers (Kuznetsova and Lee, 2001), coastal seawater and sediments (Pantoja et al., 1997; Pantoja and Lee, 1999; Liu and Liu, 2016), and an oxygen minimum zone (Pantoja et al., 2009).

However, most of these studies used LYA-labeled peptides synthesized only from alanine to estimate hydrolysis of DCAA. The alanine linkages might not be representative of peptide linkages in nature since hydrolysis rates depend on the size and chemical structure of the peptide (Pantoja and Lee, 1999; Liu et al., 2010). As a result, estimates of natural DCAA degradation may be biased. Extracellular enzymes may have a preference or specificity for particular peptide linkages, and these may vary depending on environmental conditions. For example, endopeptidases which preferentially target linkages within peptide chains may be more important during the early degradation of organic matter than exopeptidases that target the terminal ends of peptide chains (Berges and Mulholland, 2008). This is consistent with previous observations that hydrolysis rates of LYA-tetraalanine were two orders of magnitude higher than those observed for LYA-dialanine, while LYA-dialanine was the primary product of the hydrolysis of LYA-tetraalanine (Pantoja and Lee, 1999; Mulholland et al., 2009). In addition, it was recently observed that the products, but not the rates, of hydrolysis of LYA-derivatives (LYA-AVFA and LYA-ALA₄) differed from their unlabeled peptide counterparts (AVFA and ALA₄) along a salinity transect in the Mississippi River plume (Liu and Liu, 2015).

Here we compare hydrolysis of LYA-AVFA and LYA-ALA₄ to determine whether differences in peptide structures influence hydrolysis rates and pathways in natural systems. In addition, peptide hydrolysis rates are compared with uptake rates of free amino acids and dipeptides to evaluate their contributions to organic nitrogen cycling in a productive and highly dynamic estuarine environment. Finally, we compared multiple environmental parameters, e.g., DCAA and DFAA composition, abundance, uptake and hydrolysis, as well as phytoplankton production and biomass, salinity, and nutrient concentrations, during two cruises along the James River estuary to gain insights into mechanisms controlling protein degradation and recycling in estuarine systems.

2. Methods

2.1. Sample collection and hydrology in James River and lower Chesapeake Bay

The James River is a major tributary to the southern Chesapeake Bay, the largest estuarine system in North America, and contributes about 16% of the annual freshwater flow into the Bay (Pritchard, 1952) (Fig. 1). The watershed is primarily forested but includes urban and agricultural areas that contribute industrial, municipal, and agricultural

inputs. Strong tidal influences extend 150 km upstream in this shallow coastal plain estuary (Wong, 1979). Two cruises were conducted in 2008 (July 15 and August 19–20) on board the RV *Fay Slover* (Old Dominion University). Samples were collected from 11 stations along the James River over an area ranging from 1 to 29 in salinity, as well as from the southern part of the Chesapeake Bay (Stations A7 and J6), and from a station outside the Chesapeake Bay in the Atlantic Ocean (Station A8). Sampling stations were named according to the month they were occupied, July (J) or August (A) (Fig. 1). Salinity and fluorescence depth profiles were constructed and surface water (2 m) samples were collected from 8-L Niskin bottles mounted on a CTD rosette.

2.2. Dissolved amino acid analysis

Surface water samples for dissolved amino acid analysis were filtered through $0.7 \mu\text{m}$ GF/F filters immediately after collection, and stored at $-20 \text{ }^\circ\text{C}$ until analysis. DFAA concentrations were analyzed by high performance liquid chromatography (HPLC) using fluorescence detection (Lindroth and Mopper, 1979). Amino acids in thawed samples were derivatized with o-phthalaldehyde (OPA) and separated on an ODS HYPERSIL C18 column (Supelco, 150 mm, $5 \mu\text{m}$) using a gradient of 10% methanol in 0.04 M sodium acetate as solvent A and 10% 0.04 M sodium acetate in methanol as solvent B. The gradient was ramped from 10% to 60% solvent B in the first 22 min, followed by an increase to 85% solvent B in the next 17 min. The gradient was held at 85% solvent B for 2 min, and then returned to 10% B. The fluorescently labeled amino acids were detected using a Shimadzu RF-10AXL fluorometer with excitation and emission wavelengths of 330 nm and 418 nm, respectively. Amino Acid Standard H (Pierce) was used as the analytical standard. Non-protein amino acids, β -alanine (BALA) and γ -aminobutyric acid (GABA), from Sigma-Aldrich were added to Pierce standard H before injection.

THAA were determined in water samples after acid hydrolysis using a modification of the method of Reintaler et al. (2008). Dissolved samples were mixed with 12 N hydrochloric acid (trace metal grade, Sigma-Aldrich) to a final concentration of 6 N. Ascorbic acid ($10 \mu\text{mol L}^{-1}$, final concentration, Sigma-Aldrich) was added to the acidified samples to prevent oxidation. Samples were sparged with dry N_2 gas for about 15 s before sealing in glass vials with Teflon septa and vortexing. The prepared samples were hydrolyzed at $110 \text{ }^\circ\text{C}$ on a heating block for 20 h. After hydrolysis, acid was removed by drying under a stream of N_2 , and redried after adding a few drops of distilled water. Dried samples were resuspended in distilled water and methanol (v/v 6:4), and analyzed by HPLC as described above for DFAA. The hydrolysis products of asparagine and glutamine were included in aspartic acid (ASP) and glutamic acid (GLU) measurements, respectively. The analytical error of individual amino acids ranged from 1% to 16% with an average of 6%. Dissolved combined amino acids (DCAA) were calculated as the difference between THAA and DFAA.

2.3. Peptide hydrolysis

LYA derivatives of Ala₄ and AVFA and all of their possible hydrolysis products were synthesized using the method of Pantoja et al. (1997). Since neither Ala₄ nor AVFA is commercially available, they and their possible hydrolysis products were prepared by Fmoc (fluorenylmethoxycarbonyl, an amino protecting group) solid phase synthesis using an automated solid phase peptide synthesizer (Liu et al., 2010). Briefly, peptides were condensed with LYA in refluxing aqueous acetate buffer at pH 5 and $105 \text{ }^\circ\text{C}$. Raw products were purified on an ion exchange column (DOWEX, 50 W-X12, 200–400 mesh) or by HPLC. Peptide hydrolysis was measured in incubations by monitoring the loss of the fluorescently labeled peptides (LYA-Ala₄ or LYA-AVFA) and production of hydrolysis products (LYA-Ala, LYA-Ala₂, and LYA-Ala₃ for LYA-Ala₄, or LYA-ala, LYA-ala-val, and LYA-ala-val-phe for LYA-AVFA).

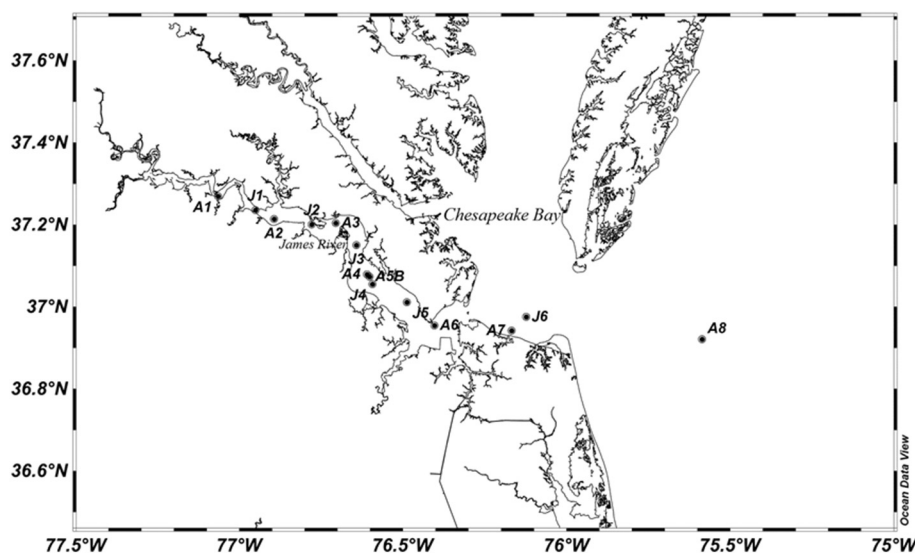


Fig. 1. Sampling stations during July (J) and August (A), 2008. Map is made by Ocean Data View.

Peptide hydrolysis was measured in whole water samples, and in water samples that had passed through 0.7 μm pre-combusted GF/F filters. Experiments were initiated immediately after sample collection by adding stock solutions of LYA-AVFA or LYA-ALA₄ to pre-combusted 40-mL borosilicate vials containing either whole or filtered surface water samples (final LYA-peptide concentration of about 100 nmol L^{-1} , equivalent to 1.2 $\mu\text{mol L}^{-1}$ carbon addition as ALA₄, and 2.0 $\mu\text{mol L}^{-1}$ carbon addition as AVFA). Vials were incubated in deckboard incubators at near-ambient temperatures and light levels, and then moved to laboratory incubators where they were held at constant temperature (24 °C). Subsamples were collected at various time intervals up to 12 h and 60 h for LYA-ALA₄ and LYA-AVFA, respectively. These time intervals were based on previous observations of LYA-ALA₄ and LYA-AVFA degradation patterns in coastal seawater. A typical LYA-ALA₄ sampling interval was 0, 0.3, 0.6, 1, 2, 4, 6, 8, 10, 12 h; while a typical LYA-AVFA sampling interval for LYA-AVFA was 0, 2, 6, 10, 12, 16, 20, 24, 28, 30 h in July and 0, 12, 24, 28, 30, 34, 37, 40, 43, 45, 54 h in August. Hydrolysis was stopped by filtering samples through 0.2 μm polycarbonate syringe filters (Millipore); the filtrate was collected into precombusted vials and immediately frozen until analysis. The loss of LYA-AVFA and LYA-ALA₄ and production of hydrolysis products were measured by HPLC using fluorescence detection with excitation and emission wavelengths of 424 and 550 nm, respectively, as described by Pantoja et al. (1997). Peptide hydrolysis rate constants in whole water (k_w) and filtered water (k_f) were calculated using only data from the first 6–12 h and assuming first order kinetics (Mulholland and Lee, 2009). Peptide hydrolysis rates (R_w) were then calculated as k_w times the measured DCAA concentrations as in Pantoja and Lee (1994).

Peptide hydrolysis rates were very low during the first 6–12 h (up to 24 h in filtered seawater, Table 2), but after the initial slow phase, the rates and rate constants increased greatly, possibly because communities adapted to the experimental conditions and increased in population, causing more rapid hydrolysis. Given the uncertainty of the cause of the increase in hydrolysis rate, we also calculated hydrolysis rate constant “potentials” (k_p) after longer incubation periods. For calculation of k_p we did not include the time (τ) of the slow phase, but used only the slope during the rapid phase. The k_p value can be viewed as the potential for the altered microbial communities to hydrolyze the supplied dissolved organic nitrogen. This potential can be estimated for whole water (k_{pw}) and for filtered water (k_{pf}).

2.4. Nutrients, chlorophyll and particulate carbon and nitrogen measurements

At each station, surface water samples were collected for nutrient analysis. Water samples were filtered through a 0.2 μm Supor cartridge filter using a peristaltic pump and collected in sterile Falcon centrifuge tubes. Separate water samples were also filtered onto pre-combusted glass fiber (GF/F) filters (0.7 μm) for analysis of chlorophyll (Chl) and total particulate carbon (TPC) and nitrogen (TPN). All samples were immediately frozen until analysis.

Concentrations of nitrite (NO_2^-), nitrate (NO_3^-), phosphate (PO_4^{3-}), and silicate (SiO_4^{4-}) were analyzed on an Astoria Pacific nutrient autoanalyzer according to manufacturer specifications using standard colorimetric methods (Parson et al., 1984). The manual phenol-hypochlorite method was used for NH_4^+ analyses (Solorzano, 1969). Total dissolved nitrogen (TDN) was analyzed as NO_3^- after persulfate oxidation (Valderrama, 1981). DON was calculated as the difference between TDN and dissolved inorganic N (DIN). Chl samples were analyzed fluorometrically within 5 d of collection (Welschmeyer, 1994). TPN and TPC samples were dried and pelletized into tin disks prior to analysis using a Europa automated nitrogen and carbon analyzer.

2.5. Uptake of organic nitrogen and inorganic nutrients

For uptake experiments, water was placed into acid-cleaned PET bottles. Incubations were initiated by adding 0.1 $\mu\text{mol } ^{15}\text{N L}^{-1}$ as highly enriched (96–99% ^{15}N and ^{13}C) dialanine or glutamic acid. While additions were targeted to achieve an atom % enrichment of approximately 10%, actual atom % enrichments varied depending on the concentration of DCAA and DFAA at stations along cruise transects. All enrichments were > 4%, a level above which reliable uptake rates can be calculated (Mulholland et al., 2009). Uptake rates were measured in triplicate. Uptake experiments were terminated after 30 min to 1 h by gently filtering the entire sample through precombusted GF/F filters, rinsed with filtered water, and frozen until analysis. Dialanine and glutamic acid uptake experiments were conducted at the same time as the hydrolysis rate experiments started, and uptake samples were filtered and a peptide hydrolysis sample collected at a common time point for direct comparison. Filters were dried at 40 °C for 2 days in an oven, then pelletized into tin discs and analyzed using a Europa 20/20 mass spectrometer equipped with an automated N and C analyzer (ANCA) preparation module. Uptake rates were calculated using a mixing model and equations from Montoya et al. (1996) and Orcutt

et al. (2001) as explained in detail in Mulholland and Lee (2009).

2.6. Statistical analysis

Principal component analysis (PCA) is a multivariate regression technique that reduces a data matrix with a large number of variables to a few variables that explain the majority of the variance in the data. PCA does not specify the underlying cause of variability, but it is used frequently in the analysis of complex organic compound datasets (e.g., Yunker et al., 1995; Ingalls et al., 2006; Goutx et al., 2007; Xue et al., 2011). PCA was performed here on two types of datasets using MYSTAT (version12, SYSTAT Software, Inc.). The first type of dataset included only the amino acid composition of the DFAA and DCAA pools. PCA(DFAA) included relative abundances (mol%) of individual DFAA at all stations, and PCA(DCAA) included relative abundances (mol%) of individual DCAA at all stations. The DFAA dataset included only ASP, GLU, SER, GLY and ALA, since other amino acids were below detection limit at more than one station. For the same reason, the DCAA data set included only ASP, GLU, THR, SER, GLY, ALA, BALA, ARG, LEU, ILE, PHE, TYR and HIS. The second type of dataset analyzed [PCA (ALL)] included all environmental parameters measured: DCAA composition, DFAA and DCAA concentrations, peptide hydrolysis potential rate constants (k_p), and time of slow phase (τ) in both whole and filtered water samples, uptake rates of amino acids and dipeptides, salinity, chlorophyll *a*, oxygen, particulate carbon and nitrogen, and nutrient concentrations. PCA graphs plotted here include both the loadings of each variance and the site scores, with values of site scores divided by five for scale. Pearson Correlation analysis was applied to determine the correlation between environmental parameters and the first two principal components from PCA (DFAA) and PCA (DCAA).

3. Results

3.1. Chlorophyll and nutrient concentrations in James River estuary and lower Chesapeake Bay

Chlorophyll concentrations ranged between 0.26 and 31.6 $\mu\text{g L}^{-1}$, and were generally higher in low salinity water and lower in higher salinity water (Table 1 and Fig. 2), except during August when there was a bloom of *Cochlodinium polykrikoides* in the lower James River estuary (Mulholland et al., 2009; Morse et al., 2011), as is common during summer months (Marshall et al. 2006; Mulholland et al., 2009). These transient blooms are sporadic and closely linked with the hydrodynamics in this region (Morse et al., 2011, 2013).

Ammonium was the most abundant form of DIN at most stations during both the July and August sampling periods (Table 1 and Fig. 2). Nitrate concentrations decreased slightly with increasing salinity, from 0.59 in the freshest water to 0.01 $\mu\text{mol L}^{-1}$ in the most saline water. A mid-estuary maximum occurred in some parameters during August just upriver from the bloom. Ammonium concentrations were 7.80 $\mu\text{mol L}^{-1}$ and nitrate concentrations were 0.17 $\mu\text{mol L}^{-1}$ at station A4, upriver of where bloom densities were highest. A much smaller mid-estuary maximum of ammonium was observed in July at a higher salinity (19.5) than in August (9.8). Concentrations of phosphate and silicate were lower at the mouth of the James River and in Chesapeake Bay than upstream with the highest concentrations observed at salinities from 5.24 to 16.0 $\mu\text{mol L}^{-1}$ (Fig. 2).

3.2. Distribution of free and combined amino acids

DCAA concentrations ranged from 0.46–1.65 $\mu\text{mol L}^{-1}$ during the study period (Table 1). These values are consistent with previous results from the Pocomoke River, a Maryland tributary of Chesapeake Bay, in May and August 1999 and 2000 (0.74–3.82 $\mu\text{mol L}^{-1}$; Mulholland et al., 2003) as well as other estuaries (Bronk, 2002, and references therein). Coffin (1989) reported DCAA concentrations 0.1 to 8 μmol

Table 1
Environmental parameters during the cruises of July and August 2008. DFAA/THAA: molecular ratio of DFAA to THAA. BLD is below the limit of analytical detection.

	Sal	Temp °C	DO mg L ⁻¹	Chl $\mu\text{g L}^{-1}$	NO ₂ ⁻ $\mu\text{mol L}^{-1}$	NO ₃ ⁻ $\mu\text{mol L}^{-1}$	NH ₄ ⁺ $\mu\text{mol L}^{-1}$	PO ₄ ³⁻ $\mu\text{mol L}^{-1}$	SiO ₄ ²⁻ $\mu\text{mol L}^{-1}$	TPC $\mu\text{mol C L}^{-1}$	TPN $\mu\text{mol N L}^{-1}$	DFAA $\mu\text{mol L}^{-1}$	DCAA $\mu\text{mol L}^{-1}$	DFAA/THAA
J1	1.25	27.41	4.78	9.59 ± 0.24	0.03 ± 0.00	0.54 ± 0.05	0.55 ± 0.2	0.70 ± 0.07	35.2 ± 17.6	65.9	10.9	0.05	0.62	0.07
J2	5.24	28.06	4.54	11.4 ± 2.0	0.02 ± 0.00	0.16 ± 0.01	1.00 ± 0.07	0.79 ± 0.00	62.9 ± 13.0	116	19.8	0.04	1.07	0.03
J3	9.82	27.28	4.69	8.40 ± 2.88	0.02 ± 0.00	0.13 ± 0.01	1.03 ± 0.18	0.87 ± 0.01	33.5 ± 4.8	75.7	15.7	0.08	0.49	0.15
J4	15.7	27.47	6.08	13.3 ± 0.6	0.01 ± 0.00	0.10 ± 0.01	1.58 ± 0.01	0.44 ± 0.08	27.4 ± 1.9	76.1	12.2	0.03	0.68	0.05
J5	19.5	25.93	5.34	5.61 ± 1.30	0.01 ± 0.01	0.02 ± 0.00	2.55 ± 0.35	0.66 ± 0.10	19.9 ± 2.5	42.3	8.80	0.06	0.90	0.06
J6	22.4	25.83	4.59	4.61 ± 0.37	0.01 ± 0.00	0.09 ± 0.00	0.86 ± 0.06	0.14 ± 0.01	18.1 ± 1.8	67.1	10.5	0.07	0.83	0.07
Aug 2008														
A1	0.94	27.66	4.75	17.4 ± 1.1	0.12 ± 0.00	0.59 ± 0.01	2.27 ± 0.76	0.50 ± 0.01	13.6 ± 0.13	90.7	15.1	0.06	1.21	0.05
A2	4.57	27.21	4.07	10.2 ± 0.3	0.40 ± 0.00	0.2 ± 0.047	0.18 ± 0.06	0.73 ± 0.03	64.0 ± 2.3	68.2	12.2	0.09	1.02	0.08
A3	9.80	27.49	4.83	7.91 ± 0.40	0.54 ± 0.00	0.04	0.15 ± 0.05	1.16 ± 0.11	83.1 ± 0.3	64.5	12.0	0.12	1.57	0.07
A4	16.0	26.47	4.05	2.95 ± 0.44	0.53 ± 0.07	0.17 ± 0.01	7.80 ± 1.02	1.27 ± 0.08	56.7 ± 5.4	36.7	6.50	0.10	1.05	0.09
A5B	20.8	26.52	7.20	31.6 ± 5.4	0.01 ± 0.00	0.08 ± 0.02	0.16 ± 0.09	0.56 ± 0.05	43.4 ± 2.8	119	16.8	0.20	1.65	0.11
A6	22.6	25.61	5.25	6.91 ± 0.00	0.01 ± 0.00	0.01 ± 0.00	0.50 ± 0.11	0.38 ± 0.11	28.3 ± 6.8	108	18.1	0.55	1.23	0.31
A7	22.9	26.27	6.34	10.0 ± 0.0	0.01 ± 0.00	0.01 ± 0.01	0.66 ± 0.20	0.20 ± 0.02	20.3 ± 1.8	175	28.1	0.25	0.77	0.24
A8	29.4	25.43	5.02	0.26 ± 0.01	BLD	0.01 ± 0.00	0.15 ± 0.08	0.03 ± 0.00	0.05 ± 0.01	10.4	1.80	0.11	0.46	0.22

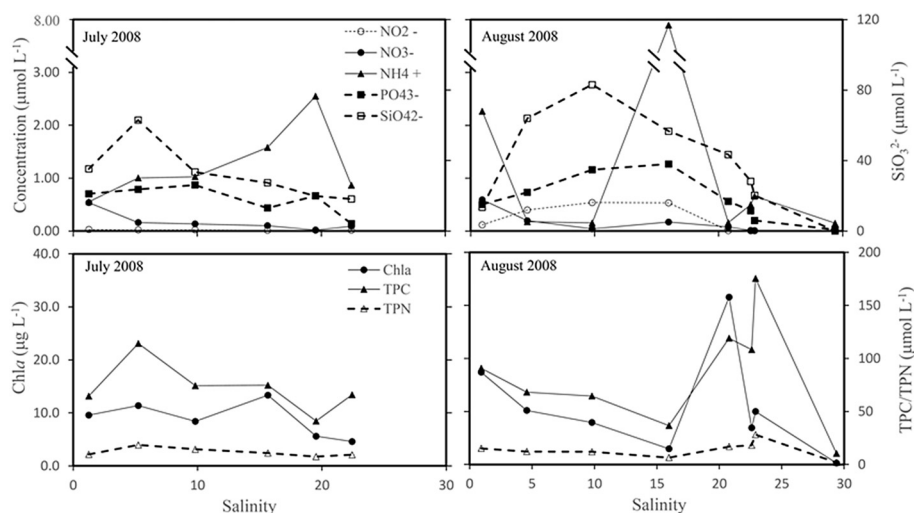


Fig. 2. Distribution of NO_2^- , NO_3^- , NH_4^+ , PO_4^{3-} , SiO_4^{2-} , Chl, TPC and TPN along the salinity transect during July and August cruises, 2008.

L^{-1} along a salinity transect in the Delaware estuary, and found that much of the DCAA were present in small (< 1000 D) peptides. The lowest DCAA concentrations were observed in August in the coastal Atlantic Ocean station near the mouth of Chesapeake Bay. These were within the range of concentrations previously observed in coastal and open ocean surface seawater (e.g., $0.2\text{--}2 \mu\text{mol L}^{-1}$ as in Lee and Bada, 1977; Kuznetsova et al., 2004; Kaiser and Benner, 2009). There was no correlation between DCAA concentrations and salinity (Table 3). Higher DCAA concentrations were observed in the area with higher chlorophyll concentrations ($r = 0.56$, $p > 0.05$, Table 3), likely because DCAA were released from living or dead cells. DCAA concentrations were also higher at stations with elevated silicate concentrations ($r = 0.55$, $p > 0.05$).

DFAA concentrations ranged from $0.03\text{--}0.55 \mu\text{mol L}^{-1}$ in surface waters (Table 1), similar to that found in the Pocomoke River ($0.07\text{--}1.34 \mu\text{mol L}^{-1}$) (Mulholland et al., 2003) and in other estuarine areas (Bronk, 2002, and references therein). The highest concentrations of DFAA were observed at the lower part of the James River estuary in August. No significant correlations were observed between DFAA concentrations and other environmental parameters, e.g. nutrients, salinity, chlorophyll, TPC or TPN (Table 3). The ratio of DFAA/THAA ranged from 0.03 to 0.31, slightly higher than observations from the Sargasso Sea where DFAA/THAA ratios of 0.04 to 0.09 have been found (Keil and Kirchman, 1999), but similar to those in coastal waters (Kuznetsova and Lee, 2002). For most stations surveyed, DFAA concentrations in both August and July were $< 20\%$ of THAA; two exceptions were from more saline stations in August where DFAA were a much higher proportion (24% and 31%) of THAA. DFAA/THAA ratios in August were slightly higher than in July (Table 1).

DFAA and DCAA compositions were similar to those reported previously from other estuarine systems (Lee and Bada, 1977; Keil and Kirchman, 1999; Kuznetsova and Lee, 2002). Aspartic acid (ASP), glutamic acid (GLU), glycine (GLY), and alanine (ALA) were the major components of the DFAA pool (Fig. 3) while GLY and ALA were the most common components of the DCAA pool in the James River estuary and adjacent Bay area. ASP and GLU were also quantitatively important components of the DCAA pool, while threonine (THR), tyrosine (TYR), valine (VAL), and leucine (LEU) accounted for smaller percentages. The non-protein amino acids, BALA, were present in DCAA at all stations surveyed during this study. More saline stations showed noticeably different DCAA compositions at lower salinity stations. The relative abundance of GLU increased with increasing salinity in both July and August. In contrast, GLY and ALA were lower at higher salinity in July, and less so in August. BALA was lower at higher salinity during both months, while GABA was higher at higher salinity only in August (Fig. 3). A detailed PCA analysis of DCAA and DFAA composition is

presented in Section 3.5.

3.3. Peptide hydrolysis

Concentrations of LYA-AVFA decreased exponentially with time in incubation experiments, and transient hydrolysis products (LYA-AVF and LYA-AV) were usually observed during this exponential degradation (Fig. 4). LYA-AV was the dominant hydrolysis product in most filtered and whole water samples by the end of the incubations. However, occasionally (e.g., stations A4 and A7 and whole water samples from A8), LYA-AVF was the most abundant hydrolysis product. Production of LYA-A was not observed in any of the experiments, likely due to the short incubation times. Similar patterns were also observed during the degradation of LYA-ALA₄, with LYA-ALA₂ being the dominant product. This peptide hydrolysis pattern has also been observed in sediments (Pantoja and Lee, 1999) and other estuarine water samples (Mulholland et al., 2002, 2003).

Hydrolysis rate constants of LYA-AVFA and LYA-ALA₄ were calculated for the first 6 to 12 h (initial slow hydrolysis phase) in both whole water (k_w) and filtered water samples (k_f) (Table 2). Relatively low rate constants that ranged from undetectable to 0.05 h^{-1} were observed, except at the bloom station in August where biomass was much higher and rate constants of 0.15 h^{-1} for LYA-AVFA and 0.03 h^{-1} for LYA-ALA₄ were observed (Table 2, Fig. 5). These rate constants were similar to those measured over similar incubation periods using LYA-ALA₄ in the Pocomoke River ($0.007\text{--}0.215 \text{ h}^{-1}$, as calculated from data in Mulholland et al., 2003). Initial rate constants measured in whole water samples were always greater than those from filtered samples. While rate constants of LYA-AVFA were always greater than those of LYA-ALA₄, k_w values for these analogs were still correlated with each other ($r = 0.77$, $p < 0.05$). There was no clear relationship between the rate constants and salinity, TPC, TPN, even though the lowest hydrolysis rate constants in whole water were observed at A8, the most saline station (Table 2). However, strong correlations were observed between chlorophyll concentrations and rate constants of both LYA-AVFA ($r = 0.90$, $p < 0.05$) and LYA-ALA₄ ($r = 0.85$, $p < 0.05$) (Table 3). Using hydrolysis rate constants, we estimated peptide hydrolysis rates by multiplying rate constants by DCAA concentrations, assuming all the combined amino acids can be hydrolyzed at the same rate as LYA-AVFA or LYA-ALA₄ (Mulholland and Lee, 2009). Peptide hydrolysis rates estimated in this way ranged from undetectable to $0.24 \mu\text{M h}^{-1}$ for LYA-AVFA, and from undetectable to $0.04 \mu\text{M h}^{-1}$ for LYA-ALA₄.

Hydrolysis potential rate constants (k_p) of LYA-AVFA calculated for the rapid hydrolysis phase, which likely reflect both the amount of biomass and the capability of microbial communities to hydrolyze the peptide bonds, were also measured in both filtered and whole water

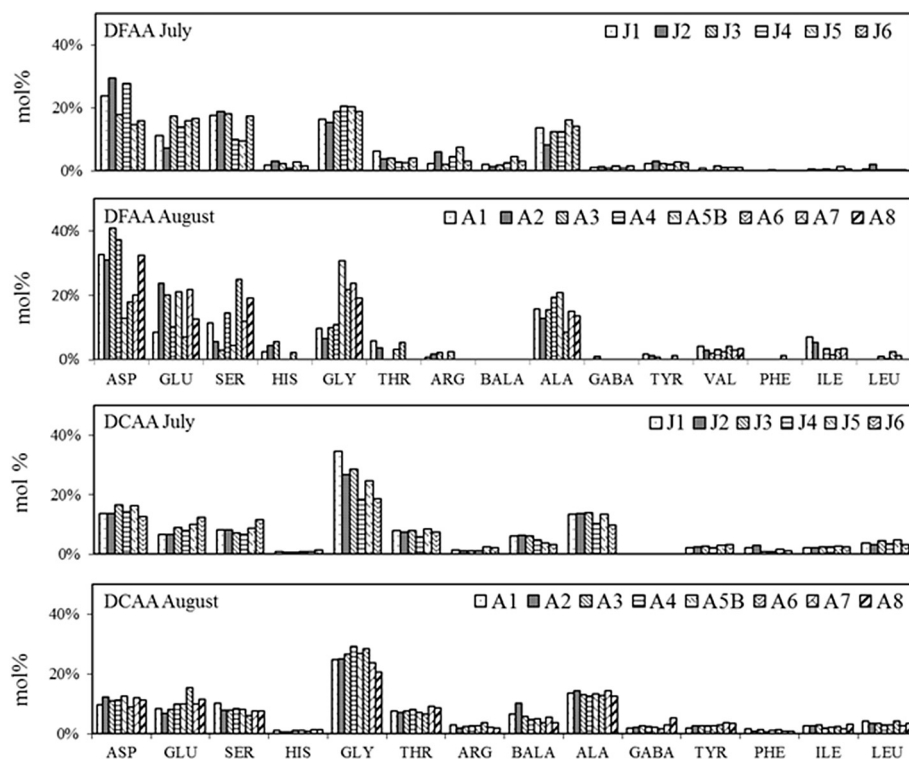


Fig. 3. Relative abundance of DFAA and DCAA in July and August 2008.

samples after the initial slow degradation phase (τ). Peptide hydrolysis k_p values for hydrolysis of LYA-AVFA ranged from $0.13\text{--}0.41\text{ h}^{-1}$ in whole water samples (k_{pw}) and from below detection to 0.55 h^{-1} in filtered water samples (k_{pf}); these k_p values were always higher than the corresponding hydrolysis rate constants (k_w and k_f) (Table 2). The correlation between hydrolysis potential rate constants of whole water samples and salinity was not strong ($r = 0.02$, $p < 0.05$; Table 3), although k_p values were generally higher in the more saline Bay stations (A7, A8, and J6) (Table 2). Although the initial phase (τ) was longer in filtered than in whole water, k_p values in whole and filtered water samples were usually similar, indicating that removal of particles does not change the k_p values in a given sample (Table 2). Due to the shorter incubation time for LYA-ALA₄ in these experiments (12 h for LYA-ALA₄ vs. 59 h for LYA-AVFA), complete loss of LYA-ALA₄ was observed only in whole water samples from the bloom station (Fig. 4), where k_{pw} values for LYA-AVFA (0.19 h^{-1}) and LYA-ALA₄ (0.18 h^{-1}) were similar (Table 2). Observed values of initial rate constants of the two analogs were similar, while the differences between k and k_p for the same analog from the same incubations were not.

3.4. Uptake of organic nitrogen

Uptake of an amino acid and a dipeptide was surveyed using two isotopically labeled compounds, glutamic acid and dialanine. Uptake rates of these two compounds have been previously measured in Chesapeake Bay and other similar environments (Dzurica et al., 1989; Keil and Kirchman, 1991; Mulholland and Lee, 2009). Our measured uptake rates (Table 2, Fig. 4) were at the lower end of rates previously reported for Chesapeake Bay, $0.002\text{--}2.22\text{ }\mu\text{MN h}^{-1}$ for glutamic acid and $0.02\text{--}1.27\text{ }\mu\text{MN h}^{-1}$ for dialanine (Mulholland et al., 2002; Mulholland and Lee, 2009). Uptake of these two organic nitrogen compounds was not correlated with salinity, but uptake of glutamic acid was strongly correlated with TPN and chlorophyll ($r = 0.73$, $p > 0.05$, Table 3). We estimated that uptake of glutamic acid and dialanine was equivalent to 42–550% of peptide hydrolysis rates in whole water samples (Table 2, Fig. 5). For most stations, the uptake rates were much higher than hydrolysis rates.

Calculation of both hydrolysis and uptake rates requires several assumptions that could result in over- or underestimates of rates. First, peptide hydrolysis rates estimated here are calculated by multiplying first-order hydrolysis rate constants by DCAA concentrations with the

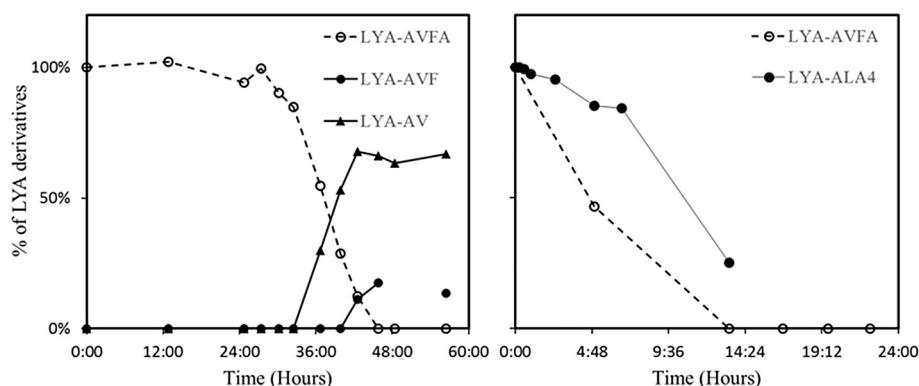


Fig. 4. Time course of hydrolysis of LYA-AVFA and production of its degradation products in filtered water samples from Sta. A3 (left); Loss of LYA-AVFA (open circles) and LYA-ALA₄ (solid circles) in whole water sample at the bloom station in August (right).

Table 2

Peptide hydrolysis and nutrient uptake parameters during July and August 2008. Hydrolysis rate constants of LYA-AVFA are calculated during the exponential decrease stage. The lag time is the length of the slow initial hydrolysis phase.

	k_w^{AVFA}	k_{pw}^{AVFA}	k_f^{AVFA}	k_{pf}^{AVFA}	k_w^{ALA4}	k_{pw}^{ALA4}	k_f^{ALA4}	τ_w	τ_f	R_w^{AVFA}	R_w^{ALA4}	R_{glu}	R_{dia}	k_{glu}	k_{dia}	%ON
	h^{-1}	h^{-1}	h^{-1}	h^{-1}	h^{-1}	h^{-1}	h^{-1}	h	h	$\mu M h^{-1}$	$\mu M h^{-1}$	$\mu MN h^{-1}$	$\mu MN h^{-1}$	h^{-1}	h^{-1}	
Jul 2008																
J1	0.03	0.21	0.00	N/A	0.01	N/A	0.00	12:36	24:00	0.02	0.01	0.01	0.03	0.11	0.09	228%
J2	0.02	0.41	0.00	N/A	0.01	N/A	0.00	8:36	24:00	0.02	0.01	0.03	0.08	0.34	0.13	550%
J3	0.03	0.17	0.00	N/A	0.01	N/A	0.00	5:53	24:00	0.01	0.01	0.03	0.03	0.25	0.11	417%
J4	0.04	0.14	0.01	N/A	0.02	N/A	0.00	8:17	24:00	0.02	0.01	0.02	0.03	0.23	0.07	214%
J5	0.02	0.23	N/A	0.14	0.02	N/A	0.00	6:25	23:17	0.01	0.01	0.02	0.01	0.20	0.02	221%
J6	0.03	0.35	N/A	0.33	0.02	N/A	0.00	8:59	24:00	0.02	0.01	0.04	0.02	0.33	0.04	225%
Aug 2008																
A1	0.05	0.24	0.01	N/A	0.02	N/A	0.00	8:13	50:00	0.06	0.02	0.02	0.03	0.20	0.05	99%
A2	0.03	0.19	0.00	N/A	0.01	N/A	0.00	6:04	50:00	0.03	0.01	0.02	0.06	0.14	0.12	299%
A3	0.02	0.14	0.00	0.16	0.01	N/A	0.00	15:40	28:41	0.03	0.01	0.01	0.05	0.11	0.06	254%
A4	0.02	0.13	0.00	0.39	0.00	N/A	0.00	5:48	12:19	0.02	0.00	0.01	0.03	0.10	0.05	197%
A5B	0.15	0.19	0.01	0.21	0.03	0.18	0.00	0:00	12:21	0.24	0.04	0.08	0.03	0.54	0.03	42%
A6	0.05	0.39	0.00	N/A	0.01	N/A	0.00	10:18	26:45	0.06	0.02	0.03	0.01	0.25	0.01	74%
A7	0.03	0.22	0.00	0.55	0.01	N/A	0.00	12:35	12:35	0.02	0.01	0.05	0.06	0.33	0.13	455%
A8	0.01	0.32	0.00	N/A	0.00	N/A	0.00	11:43	31:43	0.00	0.00	0.00	0.01	0.03	0.03	296%

k_w^{AVFA} and k_{pw}^{AVFA} are the rate constant and potential rate constant of LYA-AVFA hydrolysis in whole water.

k_f^{AVFA} and k_{pf}^{AVFA} are the rate constant and potential rate constant of LYA-AVFA hydrolysis in filtered water.

k_w^{ALA4} and k_{pw}^{ALA4} are the rate constant and potential rate constant of LYA-ALA₄ hydrolysis in whole water.

k_f^{ALA4} is the rate constant of LYA-ALA₄ hydrolysis rate of LYA-ALA₄ in filtered water.

τ_w is the lag time of LYA-AVFA hydrolysis in whole water sample.

τ_f is the lag time of LYA-AVFA hydrolysis in filtered sample.

R_w^{AVFA} is the hydrolysis rate of LYA-AVFA in whole water sample.

R_w^{ALA4} is the hydrolysis rate of LYA-ALA₄ in whole water sample.

R_{glu} and R_{dia} are the uptake rates of these compounds.

k_{glu} and k_{dia} are the uptake rate constants of these compounds.

%ON is the percentage of uptake of GLU and DiALA to R_w^{AVFA} .

assumption that all dissolved combined amino acids are available in linkages hydrolyzed at the same rate as LYA-AVFA. This obviously oversimplifies the complex nature of DCAA since differences in hydrolysis rates of various peptides have been well documented (Pantoja and Lee, 1999; Liu and Liu, 2015). Second, all hydrolysis products are assumed to be taken up at the same rate as dialanine and glutamate. This assumption neglects the potential differences in uptake rates among amino acids and oligopeptides. Consequently, our rate calculations should be considered as estimates.

3.5. Statistical analysis

PCA was performed in this study on three separate datasets. In the first data set, PCA (DFAA), the first two components explained 82% of the variance (Fig. 6). PC1 had the highest loadings of GLU and ALA, and lowest of SER. GLY was highest along the PC2 axis, and ASP was lowest. There was no clear trend with salinity, although there was a tendency for more saline stations to be generally found in the upper half of the graph and lower salinity stations in the bottom half. This placed the bloom station with the saline stations, which were generally enriched in GLU, ALA and GLY. A Pearson Correlation analysis that also included other environmental parameters indicated that PC1 had the strongest

negative correlation with k_{pw} of LYA-AVFA in whole water samples ($r = -0.73$, $p < 0.05$; Table 3), while PC2 had the strongest correlation with uptake rates of free amino acids (as UGLU, $r = 0.74$, $p < 0.05$; Table 3).

In the second dataset, PCA (DCAA), the first two components explained only 45% of the variance (Fig. 6). Amino acid composition varied from fresh to saline water along the axis of PC1 from left to right. Toward the left on the PC1 axis were BALA, ALA and GLY, while GLU and HIS were located to the right, indicating terrestrial input of more degraded organic matter from freshwater (enriched in GLY, ALA and BALA) and fresher organic matter in salt water (enriched in GLU) (Chen et al., 2004). The Pearson Correlation coefficient between salinity and PC1 was much higher ($r = 0.85$, $p < 0.05$; Table 3) than for DFAA, indicating that salinity is a primary factor influencing DCAA composition in this estuarine region. PC1 was negatively correlated with uptake rates of dialanine ($r = -0.63$, $p < 0.005$), indicating that peptide uptake plays an important role in determining DCAA composition. PC2 was characterized by positive loadings of THR, and negative loadings of LEU and ILE. Pearson Correlation analysis showed that PC2 has the highest positive correlation with hydrolysis potential rate constants of LYA-AVFA in filtered seawater ($r = 0.95$, $p < 0.05$), indicating that peptide hydrolysis may be influenced by DCAA compositions. The

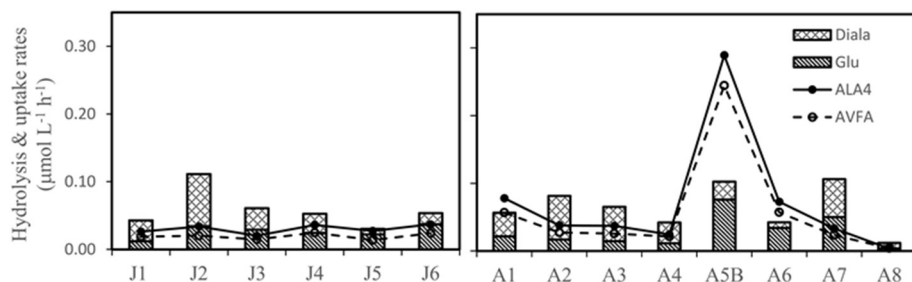


Fig. 5. Hydrolysis rates calculated from LYA-AVFA and LYA-ALA₄, and uptake rates of glutamic acid and dialanine during July (left) and August (right) cruises.

Table 3

Pearson correlation analysis of all environmental parameters at all stations. PC1 and PC2 are the first two principal components of DCAA and DFAA composition from all stations (see Fig. 6). [DFAA] and [DCAA] here represent the concentration of DFAA and DCAA respectively. The correlations in bold are significant with $r > 0.458$, $p < 0.05$, $n = 14$.

	PC1F	PC2F	PC1C	PC2C	[DFAA]	[DCAA]	FC	k_w^{AVFA}	k_w^{ALA4}	k_f	k_{pw}	k_{pf}	R_w^{AVFA}	R_w^{ALA4}	R_{glu}	R_{dia}	k_{glu}	k_{dia}
SAL	-0.14	0.54	0.85	0.09	0.44	-0.12	0.60	0.11	-0.11	0.20	0.23	0.48	0.14	0.01	0.27	-0.58	0.18	-0.52
Chla	0.34	0.37	-0.23	-0.02	0.03	0.56	-0.22	0.90	0.85	0.66	-0.20	-0.20	0.87	0.91	0.73	0.20	0.72	0.04
TPN	-0.11	0.29	-0.19	0.25	0.40	0.23	0.26	0.31	0.52	0.06	0.15	0.59	0.24	0.36	0.67	0.51	0.64	0.52
TPC	-0.08	0.35	-0.09	0.28	0.42	0.29	0.27	0.43	0.59	0.15	0.16	0.58	0.37	0.47	0.75	0.46	0.71	0.44
NO ₂ ⁻	0.54	-0.65	-0.18	-0.05	-0.13	0.41	-0.27	-0.23	-0.43	-0.58	-0.51	-0.13	-0.15	-0.22	-0.42	0.35	-0.47	0.08
NO ₃ ⁻	0.01	-0.40	-0.48	-0.03	-0.37	-0.04	-0.44	0.03	0.16	0.03	-0.12	0.12	-0.03	0.05	-0.27	0.17	-0.20	0.19
NH ₄ ⁺	0.07	-0.28	0.10	0.11	-0.18	0.00	-0.24	-0.19	-0.27	-0.29	-0.31	0.21	-0.17	-0.24	-0.28	-0.12	-0.25	-0.14
PO ₄ ³⁻	0.32	-0.42	-0.58	-0.05	-0.23	0.36	-0.45	-0.11	-0.19	-0.48	-0.51	-0.38	-0.04	-0.08	-0.25	0.37	-0.23	0.21
SiO ₄ ²⁻	0.35	-0.41	-0.55	-0.01	-0.09	0.55	-0.37	0.00	-0.09	-0.47	-0.30	-0.36	0.08	0.08	-0.03	0.66	-0.02	0.37
PC1F	1.00	0.00	-0.09	0.21	-0.38	0.37	-0.43	0.25	0.20	-0.09	-0.73	-0.61	0.29	0.29	0.09	0.23	0.02	0.04
PC2F		1.00	0.36	0.20	0.28	-0.03	0.29	0.57	0.60	0.45	0.07	-0.02	0.52	0.51	0.74	-0.43	0.70	-0.27
PC1C			1.00	0.00	0.35	-0.02	0.45	0.10	-0.04	0.27	0.26	0.45	0.11	0.04	0.20	-0.63	0.13	-0.63
PC2C				1.00	-0.30	-0.29	-0.03	-0.03	-0.07	-0.43	-0.12	0.95	-0.04	-0.13	0.23	0.38	0.19	0.52
[DFAA]					1.00	0.31	0.84	0.28	0.08	0.09	0.34	0.54	0.27	0.20	0.34	-0.26	0.21	-0.31
[DCAA]						1.00	-0.14	0.55	0.42	0.21	-0.05	-0.59	0.65	0.71	0.42	0.20	0.38	-0.27
FC							1.00	0.06	-0.22	-0.01	0.32	0.81	0.03	-0.13	0.17	-0.32	0.00	-0.17
k_w^{AVFA}								1.00	0.77	0.66	-0.11	-0.14	0.98	0.92	0.80	-0.11	0.74	-0.24
k_w^{ALA4}									1.00	0.64	-0.02	-0.18	0.71	0.88	0.80	0.01	0.83	-0.07
k_f										1.00	0.19	-0.43	0.63	0.67	0.48	-0.42	0.53	-0.47
k_{pw}											1.00	0.14	-0.09	0.01	0.13	-0.09	0.20	-0.14
k_{pf}												1.00	-0.24	-0.36	0.17	0.47	0.09	0.80
R_w^{AVFA}													1.00	0.93	0.77	-0.10	0.71	-0.30
R_w^{ALA4}														1.00	0.80	-0.01	0.79	-0.26
R_{glu}															1.00	0.08	0.97	0.02
R_{dia}																1.00	0.11	0.86
k_{glu}																	1.00	0.05
k_{dia}																		1.00

bloom station was in the middle of the PCA plot (Fig. 6).

To further investigate mechanisms influencing amino acid cycling in the area studied, a third dataset, PCA (ALL), included all parameters measured (Fig. 7). PC1 and PC2 explained only 41% of the variance. Composition of amino acids was used to determine the freshness of the organic matter (Dauwe and Middelburg, 1998). In this plot, the parameters cluster into three groups: a) open ocean stations with high salinity, low chlorophyll, but fresh organic matter clustered on the left with labile compounds like glutamic acid; b) freshwater stations with low salinity, high nutrient input, and degraded organic matter clustered on the right together with relatively refractory compounds like BALA and glycine; c) the bloom station with high Chl and high particulate nitrogen (TPN) was alone at the top of the graph. The hydrolysis potentials for both filtered and whole water were closest to the freshwater cluster. The PC1 was consistent with mixing along the salinity gradient, while the PC2 was characterized by high loading of TPN and Chl.

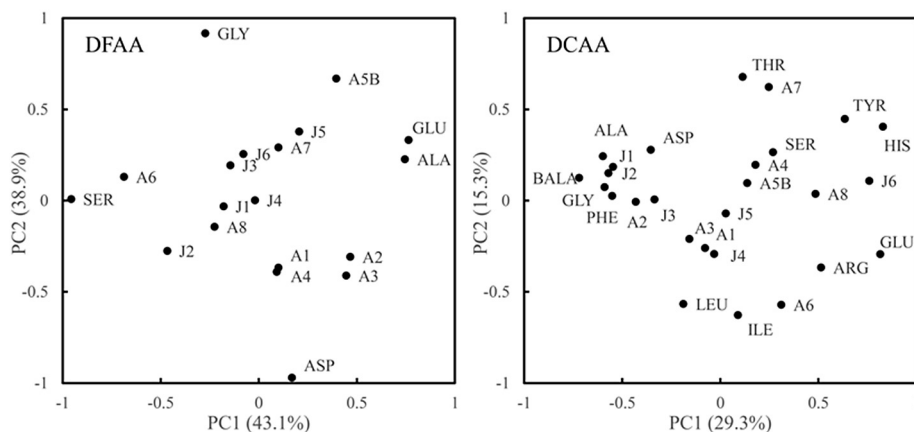


Fig. 6. Plot of first two PCs for mole% of DFAA from the July and August cruises; and first two PCs for mole% of DCAA from the July and August cruises.

4. Discussion

4.1. Comparison of LYA-AVFA and LYA-ALA₄ hydrolysis

In our study of LYA-AVFA and LYA-ALA₄ hydrolysis in estuaries, we found that hydrolysis rate constants of these two synthetic peptides followed similar patterns at all the stations sampled (Fig. 5), and rate constants of LYA-AVFA were comparable to other studies using alanine based LYA-analogs (e.g., Mulholland et al., 2002). However, rate constants were slightly higher for LYA-AVFA than for LYA-ALA₄ in whole water samples (Table 2). This could be due to structural differences between AVFA and ALA₄ as previously observed for AVFA vs. SWGA (Liu et al., 2010).

Peptide hydrolysis of both analogs follows a similar two-stage pattern with an initial slow phase (the lag phase), followed by more rapid hydrolysis as microbial biomass may increase over the course of bottle incubations (e.g., Kuznetsova and Lee, 2001; Liu et al., 2010, 2013). In our experiments, this slow hydrolysis phase was always longer in filtered samples (12 to > 50 h) than in their whole water counterparts (0–16 h) where microbial biomass was presumably higher. At the

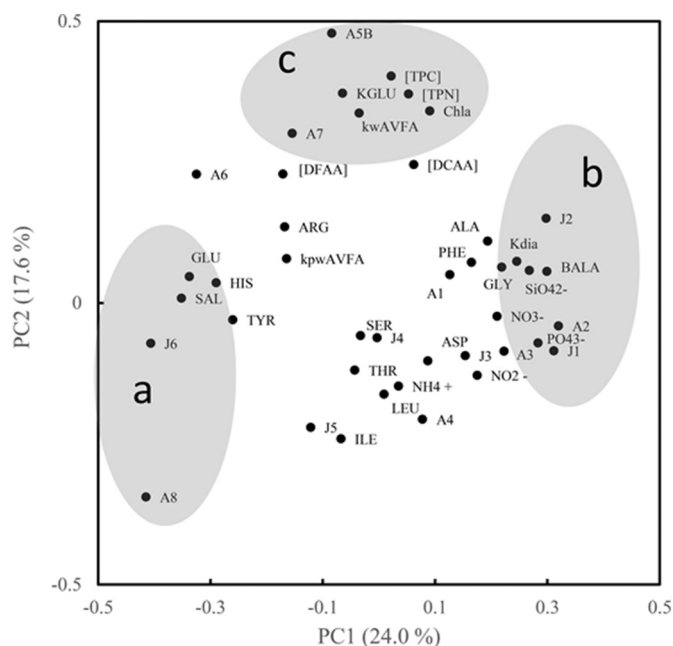


Fig. 7. Plot of first two PCs from the PCA of all environmental parameters from all sites. Shaded areas represent clusters of freshwater stations with low salinity, high nutrient input and degraded organic matter on the left (a), open ocean stations with high salinity, low chlorophyll but fresh organic matter on the right (b), and the bloom station with high chlorophyll and high particulate nitrogen (TPN) near the top of the graph (c). Other stations lie between these three groupings. [DFAA] and [DCAA]: DFAA and DCAA concentrations; k_w and k_f : peptide hydrolysis rate constants in whole and filtered water samples; KGLU and Kdia: uptake rate constants of glutamate and dialanine, SAL: salinity; Chla: chlorophyll; TPC and TPN: particulate carbon and nitrogen; NO_2^- : nitrite; NO_3^- : nitrate; PO_4^{3-} : phosphate; SiO_4^{2-} : silicate; NH_4^+ : ammonium.

August bloom station, the slow hydrolysis phase was absent or extremely short for both filtered and whole water, possibly suggesting that the initial natural community had sufficient enzymes to hydrolyze peptides at higher rates. Several possible explanations have been suggested to explain the lag time in growth observed in batch cultures, including changes in species composition, substrate and enzyme concentrations, chemical characteristics of the medium, and temperature (Stanier et al., 1986; Hills and Wright, 1994). We believe that the most likely cause of the initial slow hydrolysis phase observed in this study is related to the changing bacterial abundance and microbial community structure as a response to the addition of substrate as suggested in other peptide or protein incubations (Harvey et al., 2006; Elifantz et al., 2007; Liu et al., 2017). The bloom station in our study is a special case where both enzyme and substrate concentrations were likely elevated due to the large phytoplankton population. No lag phase was observed in whole water samples at this station in August. High peptide hydrolysis rates during the bottle experiments at the bloom station were likely associated with the high phytoplankton abundance and Chl concentrations, as has been shown previously (Kuznetsova and Lee, 2001; Mulholland and Lee, 2009).

Although LYA-derivatives are structurally more similar to natural peptides than some other fluorescent derivatives (like MUF- and MCA-labeled analogs), we should fully understand the limitations of using LYA-derivative hydrolysis as an indicator of peptide hydrolysis in aquatic environments. First, LYA-AVFA and LYA-ALA₄ are specific linkages and are not likely to be representative of the bulk DCAA pool, which is characterized by heterogeneous and complex chemical structures and bioavailabilities (Keil and Kirchman, 1993). Second, the k_p values discussed here were calculated during the exponential decrease that occurs after an initial slow phase of up to 50 h. A change in the bacterial communities and their resulting enzymatic activities would occur during this period due to changes in ambient THAA substrate and

enzymatic activity. These potential limitations may partially explain why degradation patterns of LYA-derivatives and algal proteins can be different, e.g., degradation of algal proteins can last for longer periods of time (20–50 days, Nunn et al., 2010; Moore et al., 2014). Nevertheless, LYA-AVFA and LYA-ALA₄ hydrolyze at rates comparable to amino acid and small peptide uptake (Table 2), implying that the LYA-derivatives are a reasonable indicator of peptide hydrolysis of bioavailable THAA in complicated aquatic ecosystems like James River estuary and the adjacent Bay area.

4.2. Particle associated hydrolysis and uptake of organic nitrogen in the James River estuary

Multiple lines of evidence from this work support the presence of a strong association between enzymatic hydrolysis and freshly produced particles, but not DCAA concentrations (Pantoja and Lee, 1999; Grossart et al., 2007; Mulholland et al., 2003, 2009). First, the rate constants for LYA-AVFA and LYA-ALA₄ hydrolysis during the first part of the incubations (k_w) in whole water were strongly correlated with Chl concentrations ($r = 0.90$ and $r = 0.85$, $p < 0.05$, respectively; Table 3). In contrast, the k_w of these two analogs was only weakly correlated with DCAA concentrations ($r = 0.55$ and $r = 0.42$, $p < 0.05$, respectively) and independent of salinity ($r = 0.11$ and $r = -0.11$, $p < 0.05$, respectively), implying limited influence from dissolved organic matter, terrestrial inputs or changes in microbial populations along the salinity gradient. The PCA of all environmental parameters further demonstrates that after salinity, Chl, TPC and TPN explain the second largest variance in the data (Fig. 7). Moreover, the initial slow phase of peptide hydrolysis was much longer after sample filtration and k_w was low in filtered estuarine waters, supporting the idea that tetrapeptide hydrolysis is predominantly associated with particles (Liu et al., 2015). In addition to the longer initial phase, the hydrolysis pattern was altered and LYA-AVF (and not LYA-AV) was the dominant product of peptide hydrolysis in filtered estuarine water samples (A4 and A7). Freshly produced particles provide hot spots for extracellular enzymes to access higher concentrations of substrate, which are released during cell growth and lysis. Production of extracellular enzymes is favored in locations near cell debris as a strategy to increase enzyme access to substrates (Traving et al., 2015).

The uptake rates of amino acids (as glutamic acid) were also enhanced at stations with higher Chl ($r = 0.73$, $p < 0.05$) (Table 3), similar to peptide hydrolysis rate constants, k_w . PCA of a data set that includes Chl, glutamate uptake rate constants, and the peptide hydrolysis rate constant k_w , also shows that these parameters cluster together (Fig. 7). Enhanced amino acid uptake rates may be a direct result of faster peptide hydrolysis, since preferential production of amino acids instead of dipeptides from tetrapeptide hydrolysis has been demonstrated in other eutrophic coastal waters (Liu and Liu, 2015; Liu et al., 2015). The lack of significant correlation between dialanine uptake and Chl ($r = -0.36$, $p < 0.05$, Table 3) implies that dipeptide uptake may not be as common in microbial communities as uptake of free amino acids, or that dipeptides might not be a primary hydrolysis product of DCAA. This agrees with the finding that different groups of bacteria are responsible for the assimilation of various dissolved organic substrates (Elifantz et al., 2007; Liu et al., 2017).

The lack of accumulation of large pools of DCAA and DFAA agrees with the idea of close coupling of hydrolysis and uptake (Fuhrman, 1987; Hoppe et al., 1993; Kuznetsova et al., 2004; Mulholland and Lee, 2009). This is supported by the evidence that uptake rates were higher than hydrolysis rate in most stations. In addition to peptide hydrolysis, however, excretion by phytoplankton or zooplankton is also a source of free amino acids (Johannes and Webb, 1965; Park et al., 1997). High excretion of amino acids may explain why the sum of glutamic acid and dialanine uptake rates were sometimes higher than estimated hydrolysis rates of LYA-AVFA. On the other hand, concentrations of hydrolysis products at the bloom station and another adjacent station (A6)

were high, highlighting the complexity of organic matter cycling in highly productive estuarine systems where there are multiple sources and sinks for organic compounds. Diverse input and removal processes can potentially influence both peptide hydrolysis and uptake rates, but not necessarily in the same way. Together, our results suggest that peptide hydrolysis and amino acid uptake are closely associated with particle concentrations rather than DCAA, and thus the turnover time of organic nitrogen in estuarine regions is faster in areas with more freshly produced particles.

4.3. Changes in DCAA composition and concentrations in the James River estuary and lower Chesapeake Bay

Both of the PCA analyses that included DCAA composition (Figs. 6 and 7) had first principal components that were positively correlated with salinity. This strong correlation ($r = 0.85$, $p < 0.05$, Table 3) implies that the mixing of fresh and saline water is a primary factor controlling the variation in DCAA composition, as is true of so many other dissolved constituents (Boyle et al., 1974). A likely contributor to these variations in composition is the dominant source of organic matter along the length of the estuary whether it be in-situ production of organic matter or discharge of terrestrial materials. The contribution of terrestrial inputs is greater at the freshwater end member of the estuary while at the ocean end member, the dominant sources of DCAA would be from in-situ primary production. Mixing of these estuarine end members results in a gradient of DCAA composition along the estuarine salinity gradient. Evidence for inputs of degraded terrestrial material is clear from DCAA compositional data (Fig. 3). Elevated mol% ALA and GLY were observed at the least saline stations. These two amino acids are elevated in terrestrial material (e.g., Pasqual et al., 2011) as well as in more degraded samples of seawater and marine particles (Lee et al., 2000; Yamashita and Tanoue, 2003), and particularly GLY is considered to be an indicator of degradation (Ingalls et al., 2003; Dauwe and Middelburg, 1998). The appearance of the non-protein amino acids GABA and BALA are also considered indicators of amino acid degradation during early diagenesis (Lee and Cronin, 1982; Cowie and Hedges, 1994; Ingalls et al., 2003). However, in the James River estuary, GABA and BALA were not correlated with low salinity (Fig. 3), suggesting that the use of amino acid composition as a degradation index should be used with caution in estuarine areas with multiple sources of organic matter input.

Even though DCAA composition was strongly correlated with salinity (Fig. 7), there was no correlation ($r = -0.12$, $p < 0.05$; Table 3) observed between DCAA concentrations and salinity. The absence of correlation indicates that the concentrations of DCAA are not controlled by conservative mixing of fresh and saline end members in the James River estuary. The absence of correlation between concentrations of labile organic components and salinity is frequently observed in estuaries and is thought to be due to their short retention time in the water column (He et al., 2010). Biological hot spots enriched with amino acids have been observed in coastal shelf waters (Shen et al., 2016), suggesting the importance of in-situ primary production as a source of amino acids in coastal regions. This input has been largely underestimated in the past (Bianchi et al., 2004; Davis et al., 2009), probably because concentrations are low and recycling rates are rapid. Pearson Correlation analysis suggests a correlation between DCAA concentrations (but not composition), chlorophyll concentrations ($r = 0.56$, $p < 0.05$; Table 3), and peptide hydrolysis, k_w^{AVFA} ($r = 0.55$, $p < 0.05$) throughout the estuary, suggesting that in situ primary production and consequent elevated enzymatic activity might be important in controlling the DCAA concentrations. Thus, accumulation of DCAA at the bloom station would result from decoupling between enzymatic hydrolysis and uptake of small nitrogen molecules. In areas with lower primary production, hydrolysis and uptake would be more tightly coupled so that their influence on nitrogen cycling was not observed in DCAA distributions along the transect.

Our study in the James River estuary explored organic nitrogen cycling in a complex estuarine environment. The distribution of DCAA and DFAA in the estuary was dynamic and influenced by input from in-situ production and removal from peptide hydrolysis. Compositional changes of DCAA and DFAA demonstrate the mixing of two sources of organic nitrogen along the salinity transect: terrestrial material and in-situ production. Peptide hydrolysis and uptake rates of amino acids and small peptides suggest more rapid turnover of enzymatically available organic nitrogen in regions with elevated phytoplankton biomass.

Acknowledgements

We thank the crew of R/V Slover for help with sampling. We also thank Peter Bernhardt for assistance in sample analysis. This research was supported by the U.S. NSF Chemical Oceanography Program (OCE-0726632). Funding from the Fundamental Research Funds for the Central Universities, China (20720160112) aided completion of the manuscript.

References

- Arnosti, C., 2004. Speed bumps and barricades in the carbon cycles: substrate structural effects on carbon cycling. *Mar. Chem.* 92, 263–273. <http://dx.doi.org/10.1016/j.marchem.2004.06.030>.
- Arnosti, C., 2011. Microbial extracellular enzymes and the marine carbon cycle. *Annu. Rev. Mar. Sci.* 3, 401–425. <http://dx.doi.org/10.1146/annurev-marine-120709-142731>.
- Berges, J.A., Mulholland, M., 2008. Enzymes and cellular N cycling. In: Capone, D.G., Bronk, D.A., Mulholland, M.R., Carpenter, E.J. (Eds.), *Nitrogen in the Marine Environment*. Elsevier/Academic, pp. 1385–1444.
- Berman, T., Bronk, D.A., 2003. Dissolved organic nitrogen: a dynamic participant in aquatic ecosystems. *Aquat. Microb. Ecol.* 31, 279–305. <http://dx.doi.org/10.3354/ame031279>.
- Bianchi, T.S., Filley, T., Dria, K., Hatcher, P.G., 2004. Temporal variability in sources of dissolved organic carbon in the lower Mississippi River. *Geochim. Cosmochim. Acta* 68, 959–967. <http://dx.doi.org/10.1016/j.gca.2003.07.011>.
- Billen, G., Fontigny, A., 1987. Dynamics of a *Phaeocystis*-dominated spring bloom in Belgian coastal waters. II. Bacterioplankton dynamics. *Mar. Ecol. Prog. Ser.* 37, 249–257. <http://dx.doi.org/10.3354/meps037249>.
- Boyle, E., Collier, A.T., Dengler, A.T., Edmond, J.M., Ng, A.C., Stallard, R.F., 1974. On the chemical mass-balance in estuaries. *Geochim. Cosmochim. Acta* 38, 1719–1728. [http://dx.doi.org/10.1016/0016-7037\(74\)90188-4](http://dx.doi.org/10.1016/0016-7037(74)90188-4).
- Bronk, D.A., 2002. Dynamics of DON. In: Carlson, C., Hansell, D. (Eds.), *Biogeochemistry of Marine Dissolved Organic Matter*. Academic Press, San Diego, pp. 153–247.
- Chen, J.F., Li, Y., Yin, K.D., Jin, H.Y., 2004. Amino acids in the Pearl River Estuary and adjacent waters: origins, transformation and degradation. *Cont. Shelf Res.* 24, 1877–1894. <http://dx.doi.org/10.1016/j.csr.2004.06.013>.
- Chrost, R.J., 1991. Environmental control of the synthesis and activity of aquatic microbial ectoenzymes. In: Chrost, R.J. (Ed.), *Microbial Enzymes in Aquatic Environments*. Springer-Verlag, New York, pp. 29–59.
- Coffin, R.B., 1989. Bacterial uptake of dissolved free and combined amino acids in the estuarine waters. *Limnol. Oceanogr.* 34, 531–542. <http://dx.doi.org/10.4319/lo.1989.34.3.0531>.
- Cowie, G.L., Hedges, J.I., 1994. Biochemical indicators of diagenetic alteration in organic-matter mixtures. *Nature* 369, 304–307. <http://dx.doi.org/10.1038/369304a0>.
- Dauwe, B., Middelburg, J.J., 1998. Amino acids and hexosamines as indicators of organic matter degradation state in North Sea sediments. *Limnol. Oceanogr.* 43, 782–798.
- Davis, J., Kaiser, K., Benner, R., 2009. Amino acid and amino sugar yields and compositions as indicators of dissolved organic matter diagenesis. *Org. Geochem.* 40, 343–352. <http://dx.doi.org/10.1016/j.orggeochem.2008.12.003>.
- Dzurica, S., Lee, C., Cosper, E.M., Carpenter, E.J., 1989. Role of environmental variables, specifically organic compounds and micronutrients, in the growth of the *Chrysochloris aureococcus anophagefferens*. In: Cosper, E.M., Bricelj, V.M., Carpenter, E.J. (Eds.), *Novel Phytoplankton Blooms. Coastal and Estuarine Studies*, vol. 35 Springer-Verlag, Berlin.
- Elifantz, H., Dittel, A.I., Cottrell, M.T., Kirchman, D.L., 2007. Dissolved organic matter assimilation by heterotrophic bacterial groups in the western Arctic Ocean. *Aquat. Microb. Ecol.* 50, 39–49. <http://dx.doi.org/10.3354/ame01145>.
- Fuhrman, J., 1987. Close coupling between release and uptake of dissolved free amino acids in seawater studied by an isotope dilution approach. *Mar. Ecol. Prog. Ser.* 37, 45–52. <http://dx.doi.org/10.3354/meps037045>.
- Goutx, M., Wakeham, S.G., Lee, C., Duflos, M., Guigue, C., Liu, Z., Moriceau, B., Sempere, R., Tedetti, M., Xue, J., 2007. Composition and degradation of marine particles with different settling velocities in the northwestern Mediterranean sea. *Limnol. Oceanogr.* 52, 1645–1664. <http://dx.doi.org/10.4319/lo.2007.52.4.1645>.
- Grace, B., Bianchi, T., 2010. Sorption and desorption dynamics of bulk dissolved organic matter and amino acids in the Mississippi River plume – a microcosm study. *Mar. Freshw. Res.* 61, 1067–1081. <http://dx.doi.org/10.1071/mf09181>.
- Grossart, H.P., Tang, K.W., Kiorboe, T., Ploug, H., 2007. Comparison of cell-specific

- activity between free-living and attached bacteria using isolates and natural assemblages. *FEMS Microbiol. Lett.* 266, 194–200. <http://dx.doi.org/10.1111/j.1574-6968.2006.00520.x>.
- Guldberg, L.B., Finster, K., Jorgensen, N.O.G., Middelboe, M., Lomstein, B.A., 2002. Utilization of marine sedimentary dissolved organic nitrogen by native anaerobic bacteria. *Limnol. Oceanogr.* 47, 1712–1722.
- Harvey, H.R., Dyda, R.Y., Kirchman, D.L., 2006. Impact of DOM composition on bacterial lipids and community structure in estuaries. *Aquat. Microb. Ecol.* 42, 105–117. <http://dx.doi.org/10.3354/ame042105>.
- He, B., Dai, M., Zhai, W., Wang, L., Wang, K., Chen, J., Lin, J., Han, A., Xu, Y., 2010. Distribution, degradation and dynamics of dissolved organic carbon and its major compound classes in the Pearl River estuary, China. *Mar. Chem.* 119 (1), 52–64. <http://dx.doi.org/10.1016/j.marchem.2009.12.006>.
- Hills, B.P., Wright, K.M., 1994. A new model for bacterial growth in heterogeneous systems. *J. Theor. Biol.* 168, 31–41. <http://dx.doi.org/10.1006/jtbi.1994.1085>.
- Hollibaugh, J.T., Azam, F., 1983. Microbial degradation of dissolved proteins in seawater. *Limnol. Oceanogr.* 28, 1104–1116.
- Hoppe, H.G., 1983. Significance of exoenzymatic activities of the ecology of brackish water – measurements by means of methylumbelliferyl substrates. *Mar. Ecol. Prog. Ser.* 11, 299–308. <http://dx.doi.org/10.3354/meps011299>.
- Hoppe, H.G., Ducklow, H., Karasch, B., 1993. Evidence for dependency of bacterial growth on enzymatic-hydrolysis of particulate organic matter in the mesopelagic ocean. *Mar. Ecol. Prog. Ser.* 93, 277–283. <http://dx.doi.org/10.3354/meps093277>.
- Hoppe, H.G., Armosti, C., Herndl, G., 2002. Ecological significance of bacterial enzymes in the marine environment. In: Burns, R., Dick, R. (Eds.), *Enzymes in the Environment: Activity, Ecology and Applications*. Marcel Dekker, New York, pp. 73–107.
- Ingalls, A.E., Lee, C., Wakeham, S.G., Hedges, J.I., 2003. The role of biominerals in the sinking flux and preservation of amino acids in the Southern Ocean along 170 degrees W. *Deep Sea Res. II* 50, 713–738. [http://dx.doi.org/10.1016/S0967-0645\(02\)00592-1](http://dx.doi.org/10.1016/S0967-0645(02)00592-1).
- Ingalls, A.E., Liu, Z.F., Lee, C., 2006. Seasonal trends in the pigment and amino acid compositions of sinking particles in biogenic CaCO₃ and SiO₂ dominated regions of the Pacific sector of the Southern Ocean along 170 degrees W. *Deep Sea Res I* 53, 836–859. <http://dx.doi.org/10.1016/j.dsr.2006.01.004>.
- Johannes, R.E., Webb, K.L., 1965. Release of dissolved amino acids by marine zooplankton. *Science* 150, 76–77. <http://dx.doi.org/10.1126/science.150.3692.76>.
- Kaiser, K., Benner, R., 2009. Biochemical composition and size distribution of organic matter at the Pacific and Atlantic time-series stations. *Mar. Chem.* 113, 63–77. <http://dx.doi.org/10.1016/j.marchem.2008.12.004>.
- Keil, R.G., Kirchman, D.L., 1991. Dissolved combined amino acids in marine waters as determined by a vapor-phase hydrolysis method. *Mar. Chem.* 33, 243–259. [http://dx.doi.org/10.1016/0304-4203\(91\)90070-d](http://dx.doi.org/10.1016/0304-4203(91)90070-d).
- Keil, R.G., Kirchman, D.L., 1993. Dissolved combined amino acids: chemical form and utilization by marine bacteria. *Limnol. Oceanogr.* 38, 1256–1270.
- Keil, R.G., Kirchman, D.L., 1999. Utilization of dissolved protein and amino acids in the northern Sargasso Sea. *Aquat. Microb. Ecol.* 18, 293–300. <http://dx.doi.org/10.3354/ame018293>.
- Kirchman, D.L., Hodson, R., 1984. Inhibition by peptides of amino acid uptake by bacterial populations in natural waters: implications for the regulation of amino acid transport and incorporation. *Appl. Environ. Microbiol.* 47, 624–631.
- Kroer, N., Jorgensen, N.O.G., Coffin, R.B., 1994. Utilization of dissolved nitrogen by heterotrophic bacterioplankton: a comparison of three ecosystems. *Appl. Environ. Microbiol.* 60, 4116–4123.
- Kuznetsova, M., Lee, C., 2001. Enhanced extracellular enzymatic peptide hydrolysis in the sea-surface microlayer. *Mar. Chem.* 73, 319–332. [http://dx.doi.org/10.1016/S0304-4203\(00\)00116-x](http://dx.doi.org/10.1016/S0304-4203(00)00116-x).
- Kuznetsova, M., Lee, C., 2002. Dissolved free and combined amino acids in nearshore seawater, sea surface microlayers and foams: influence of extracellular hydrolysis. *Aquat. Sci.* 64, 252–268. <http://dx.doi.org/10.1007/s00027-002-8070-0>.
- Kuznetsova, M., Lee, C., Aller, J., Frew, N., 2004. Enrichment of amino acids in the sea surface microlayer at coastal and open ocean sites in the North Atlantic Ocean. *Limnol. Oceanogr.* 49, 1605–1619.
- Lee, C., Bada, J.L., 1977. Dissolved amino acids in equatorial Pacific, Sargasso Sea, and Biscayne Bay. *Limnol. Oceanogr.* 22, 502–510. <http://dx.doi.org/10.4319/lo.1977.22.3.0502>.
- Lee, C., Cronin, C., 1982. The vertical flux of particulate organic nitrogen in the sea – decomposition of amino acids in the Peru upwelling area and the equatorial Atlantic. *J. Mar. Res.* 40, 227–251.
- Lee, C., Wakeham, S.G., Hedges, J.I., 2000. Composition and flux of particulate amino acids and chlorophylls in equatorial Pacific seawater and sediments. *Deep-Sea Res. I Oceanogr. Res. Pap.* 47, 1535–1568. [http://dx.doi.org/10.1016/S0967-0637\(99\)00116-8](http://dx.doi.org/10.1016/S0967-0637(99)00116-8).
- Lindroth, P., Mopper, K., 1979. High performance liquid chromatographic determination of subpicomole amounts of amino acids by precolumn fluorescence derivatization with o-phthalaldehyde. *Anal. Chem.* 51, 1667–1674. <http://dx.doi.org/10.1021/ac50047a019>.
- Liu, S., Liu, Z., 2015. Comparing extracellular enzymatic hydrolysis between plain peptides and their corresponding analogs in the northern Gulf of Mexico Mississippi River plume. *Mar. Chem.* 177, 398–407. <http://dx.doi.org/10.1016/j.marchem.2015.06.021>.
- Liu, Z., Liu, S., 2016. High phosphate concentrations accelerate bacterial peptide decomposition in hypoxic bottom waters of the northern Gulf of Mexico. *Environ. Sci. Technol.* 50, 676–684. <http://dx.doi.org/10.1021/acs.est.5b03039>.
- Liu, Z., Kobiela, M., McKee, G.A., Tang, T., Lee, C., Mulholland, M.R., Hatcher, P.G., 2010. The effect of chemical structure on the hydrolysis of tetrapeptides along a river-to-ocean transect: AVFA and SWGA. *Mar. Chem.* 119, 108–120. <http://dx.doi.org/10.1016/j.marchem.2010.01.005>.
- Liu, Z., Liu, S., Liu, J., Gardner, W.S., 2013. Differences in peptide decomposition rates and pathways between hypoxic and oxic coastal environments. *Mar. Chem.* 157, 67–77. <http://dx.doi.org/10.1016/j.marchem.2013.08.003>.
- Liu, S., Riesen, A., Liu, Z., 2015. Differentiating the role of different-sized microorganisms in peptide decomposition during incubations using size-fractionated coastal seawater. *J. Exp. Mar. Bio. Ecol.* 472, 97–106. <http://dx.doi.org/10.1016/j.jembe.2015.07.004>.
- Liu, S., Wawrik, B., Liu, Z., 2017. Different bacterial communities involved in peptide decomposition between normoxic and hypoxic coastal waters. *Front. Microbiol.* 8, 1–17. <http://dx.doi.org/10.3389/fmicb.2017.00353>.
- Montoya, J.P., Voss, M., Kahler, P., Capone, D., 1996. A simple, high-precision, high-sensitivity tracer assay for N₂ fixation. *Appl. Environ. Microbiol.* 62, 986–993.
- Marshall, H.G., Lacouture, R.V., Buchanan, C., Johnson, J.M., 2006. Phytoplankton assemblages associated with water quality and salinity regions in Chesapeake Bay, USA. *Estuar. Coast. Shelf Sci.* 69, 10–18. <http://dx.doi.org/10.1016/j.ecss.2006.03.019>.
- Moore, E.K., Harvey, H.R., Faux, J.F., Goodlett, D.R., Nunn, B.L., 2014. Protein recycling in Bering Sea algal incubation. *Mar. Ecol. Prog. Ser.* 515, 45–59.
- Morse, R.E., Shen, J., Blanco-Garcia, J.L., Hunley, W.S., Fentress, S., Wiggins, M., Mulholland, M.R., 2011. Environmental and physical controls on the formation and transport of blooms of the dinoflagellate *Cochlodinium polykrikoides* Margalef in lower Chesapeake Bay and its tributaries. *Estuar. Coasts* 34, 1006–1025. <http://dx.doi.org/10.1007/s12237-011-9398-2>.
- Morse, R.E., Mulholland, M.R., Hunley, W.S., Fentress, S., Wiggins, M., Blanco-Garcia, J.L., 2013. Controls on the initiation and development of blooms of the dinoflagellate *Cochlodinium polykrikoides* Margalef in lower Chesapeake Bay and its tributaries. *Harmful Algae* 28, 71–82. <http://dx.doi.org/10.1016/j.hal.2013.05.013>.
- Mulholland, M.R., Lee, C., 2009. Peptide hydrolysis and the uptake of dipeptides by phytoplankton. *Limnol. Oceanogr.* 54, 856–868. <http://dx.doi.org/10.4319/lo.2009.54.3.0856>.
- Mulholland, M.R., Lomas, M.W., 2008. Nitrogen uptake and assimilation. In: Capone, D.G. (Ed.), *Nitrogen in the Marine Environment*. Academic Press, Burlington, pp. 303–384.
- Mulholland, M.R., Gobler, C.J., Lee, C., 2002. Peptide hydrolysis, amino acid oxidation, and nitrogen uptake in communities seasonally dominated by *Aureococcus anophagefferens*. *Limnol. Oceanogr.* 47, 1094–1108.
- Mulholland, M.R., Lee, C., Glibert, P.M., 2003. Extracellular enzyme activity and uptake of carbon and nitrogen along an estuarine salinity and nutrient gradient. *Mar. Ecol. Prog. Ser.* 258, 3–17. <http://dx.doi.org/10.3354/meps258003>.
- Mulholland, M.R., Morse, R.E., Boneillo, G.E., Bernhardt, P.W., Filippino, K.C., Procise, L.A., Blanco-Garcia, J.L., Marshall, H.G., Egerton, T.A., Hunley, W.S., Moore, K.A., Berry, D.L., Gobler, C.J., 2009. Understanding causes and impacts of the dinoflagellate, *Cochlodinium polykrikoides*, blooms in the Chesapeake Bay. *Estuar. Coasts* 32, 734–747. <http://dx.doi.org/10.1007/s12237-009-9169-5>.
- Nunn, B.L., Ting, Y.S., Malmstroem, L., Tsai, Y.S., Squier, A., Goodlett, D.R., Harvey, H.R., 2010. The path to preservation: using proteomics to decipher the fate of diatom proteins during microbial degradation. *Limnol. Oceanogr.* 55, 1790–1804.
- Orcutt, K.M., Lipschultz, F., Gundersen, K., Arimoto, R., Michaels, A.F., Knap, A.H., Gallon, J.R., 2001. A seasonal study of the significance of N₂ fixation by *Trichodesmium* spp. at Bermuda Atlantic time-series study (BATS) site. *Deep-Sea Res. II Top. Stud. Oceanogr.* 48, 1583–1608. [http://dx.doi.org/10.1016/S0967-0645\(00\)00157-0](http://dx.doi.org/10.1016/S0967-0645(00)00157-0).
- Pantoja, S., Lee, C., 1994. Cell-surface oxidation of amino acids in seawater. *Limnol. Oceanogr.* 39, 1718–1726.
- Pantoja, S., Lee, C., 1999. Peptide decomposition by extracellular hydrolysis in coastal seawater and salt marsh sediment. *Mar. Chem.* 63, 273–291. [http://dx.doi.org/10.1016/S0304-4203\(98\)00067-x](http://dx.doi.org/10.1016/S0304-4203(98)00067-x).
- Pantoja, S., Lee, C., Marecek, J.F., 1997. Hydrolysis of peptides in seawater and sediment. *Mar. Chem.* 57, 25–40. [http://dx.doi.org/10.1016/S0304-4203\(97\)00003-0](http://dx.doi.org/10.1016/S0304-4203(97)00003-0).
- Pantoja, S., Rossel, P., Castro, R., Cuevas, L.A., Daneri, G., Cordova, C., 2009. Microbial degradation rates of small peptides and amino acids in the oxygen minimum zone of Chilean coastal waters. *Deep-Sea Res. II Top. Stud. Oceanogr.* 56, 1019–1026. <http://dx.doi.org/10.1016/j.dsr.2.2008.09.007>.
- Park, J.C., Aizaki, M., Fukushima, T., Otsuki, A., 1997. Production of labile and refractory dissolved organic carbon by zooplankton excretion: an experimental study using large outdoor continuous flow through ponds. *Can. J. Fish. Aquat. Sci.* 54, 434–443. <http://dx.doi.org/10.1139/cjfas-54-2-434>.
- Parson, T.R., Maita, Y., Lalli, C.M., 1984. *A Manual of Chemical and Biological Method for Seawater Analysis*. Pergamon, Oxford.
- Pasqual, C., Lee, C., Goñi, M., Tesi, T., Sanchez-Vidal, A., Calafat, A., Canals, M., Heussner, S., 2011. Use of organic biomarkers to trace the transport of marine and terrigenous organic matter through the southwestern canyons of the Gulf of Lion. *Mar. Chem.* 126, 1–12. <http://dx.doi.org/10.1016/j.marchem.2011.03.001>.
- Payne, J.W., 1980. Transport and utilization of peptides by bacterial. In: Payne, J.W. (Ed.), *Microorganisms and Nitrogen Sources*. John Wiley and Sons, New York, pp. 211–256.
- Pritchard, D.W., 1952. Salinity distribution and circulation in the Chesapeake Bay estuarine system. *J. Mar. Res.* 11, 106–123.
- Reinthal, T., Sintès, E., Herndl, G.J., 2008. Dissolved organic matter and bacterial production and respiration in the sea-surface microlayer of the open Atlantic and the western Mediterranean Sea. *Limnol. Oceanogr.* 53, 122–136. <http://dx.doi.org/10.4319/lo.2008.53.1.0122>.
- Repeta, D.J., 2014. Chemical composition and cycling of dissolved organic matter. In: Carlson, C., Hansell, D. (Eds.), *Biogeochemistry of Marine Dissolved Organic Matter*. Academic, San Diego, pp. 21–63.
- Rosenstock, B., Zwisler, W., Simon, M., 2005. Bacterial consumption of humic and non-humic low and high molecular weight DOM and the effect of solar irradiation on the

- turnover of labile DOM in the Southern Ocean. *Microb. Ecol.* 50, 90–101. <http://dx.doi.org/10.1007/s00248-004-0116-5>.
- Shen, Y., Fichot, C.G., Liang, S.K., Benner, R., 2016. Biological hot spots and the accumulation of marine dissolved organic matter in a highly productive ocean margin. *Limnol. Oceanogr.* 61, 1287–1300. <http://dx.doi.org/10.1002/lno.10290>.
- Solorzano, L., 1969. Determination of ammonia in natural waters by the phenylhypochlorite method. *Limnol. Oceanogr.* 14, 799–801.
- Somville, M., Billen, G., 1983. A method for determining exoproteolytic activity in natural waters. *Limnol. Oceanogr.* 28, 190–193.
- Stanier, R.Y., Ingraham, J.L., Wheelis, M.L., Painter, P.R., 1986. *Microbial World*, 5th ed. Prentice-Hall, Englewood Cliffs, NJ, pp. 689.
- Traving, S.J., Thygesen, U.H., Riemann, L., Stedmon, C.A., 2015. A model of extracellular enzymes in free-living microbes: which strategy pays off? *Appl. Environ. Microbiol.* 81, 7385–7393. <http://dx.doi.org/10.1128/AEM.02070-15>.
- Valderrama, J.C., 1981. The simultaneous analysis of total nitrogen and total phosphorus in natural waters. *Mar. Chem.* 10 (2), 109–122.
- Weiss, M.S., Abele, U., Weckesser, J., Welte, W., Schiltz, E., Schulz, G.E., 1991. Molecular architecture and electrostatic properties of a bacterial porin. *Science* 254, 1627–1630. <http://dx.doi.org/10.1126/science.1721242>.
- Welschmeyer, N.A., 1994. Fluorometric analysis of chlorophyll a in the presence of chlorophyll b and pheopigments. *Limnol. Oceanogr.* 39, 1985–1992. <http://dx.doi.org/10.4319/lo.1994.39.8.1985>.
- Williams, P.J.L., Berman, T., Holm-Hansen, O., 1976. Amino acid uptake and respiration by marine heterotrophs. *Mar. Biol.* 35, 41–47. <http://dx.doi.org/10.1007/BF00386673>.
- Wong, G.T.F., 1979. Alkalinity and pH in the southern Chesapeake Bay and the James River estuary. *Limnol. Oceanogr.* 24, 970–977. <http://dx.doi.org/10.4319/lo.1979.24.5.0970>.
- Xue, J., Lee, C., Wakeham, S.G., Armstrong, R.A., 2011. Using principal components analysis (PCA) with cluster analysis to study the organic geochemistry of sinking particles in the ocean. *Org. Geochem.* 42, 356–367. <http://dx.doi.org/10.1016/j.orggeochem.2011.01.012>.
- Yamashita, Y., Tanoue, E., 2003. Distribution and alteration of amino acids in bulk DOM along a transect from bay to oceanic waters. *Mar. Chem.* 82, 145–160. [http://dx.doi.org/10.1016/S0304-4203\(03\)00049-5](http://dx.doi.org/10.1016/S0304-4203(03)00049-5).
- Yunker, M.B., Macdonald, R.W., Veltkamp, D.J., Cretney, W.J., 1995. Terrestrial and marine biomarkers in a seasonally ice-covered Arctic estuary – integration of multivariate and biomarker approaches. *Mar. Chem.* 49, 1–50. [http://dx.doi.org/10.1016/0304-4203\(94\)00057-K](http://dx.doi.org/10.1016/0304-4203(94)00057-K).